ISSN 1674-1056
http://cpb.iphy.ac.cn
http://iopscience.iop.org/cpb
中国物理 B
Chinese Physics
中国物理
Chinese Physics B

Measurement of the bulk and surface bands in Dirac line-node semimetal ZrSiS

Guang-Hao Hong(洪光昊), Cheng-Wei Wang(王成玮), Juan Jiang(姜娟), Cheng Chen(陈成), Sheng-Tao Cui(崔胜涛), Hai-Feng Yang(杨海峰), Ai-Ji Liang(梁爱基), Shuai Liu(刘帅), Yang-Yang Lv(吕洋洋), Jian Zhou(周健), Yan-Bin Chen(陈延彬), Shu-Hua Yao(姚淑华), Ming-Hui Lu(卢明辉), Yan-Feng Chen(陈延峰), Mei-Xiao Wang(王美晓), Le-Xian Yang(杨乐仙), Zhong-Kai Liu(柳仲楷), Yu-Lin Chen(陈宇林)
Citation: Chin. Phys. B . 2018, 27(1): 017105. **doi:** 10.1088/1674-1056/27/1/017105

Journal homepage: http://cpb.iphy.ac.cn; http://iopscience.iop.org/cpb

What follows is a list of articles you may be interested in

Control of topological phase transitions in Dirac semimetal films by exchange fields

Fei Yang(杨菲), Hai-Long Wang(王海龙), Hui Pan(潘晖)
Chin. Phys. B . 2017, 26(1): 017102. **doi:** 10.1088/1674-1056/26/1/017102

Electronic structure of O-doped SiGe calculated by DFT+*U* method

Zong-Yan Zhao(赵宗彦), Wen Yang(杨雯), Pei-Zhi Yang(杨培志)
Chin. Phys. B . 2016, 25(12): 127101. **doi:** 10.1088/1674-1056/25/12/127101

Band offsets engineering at $Cd_xZn_{1-x}S/Cu_2ZnSnS_4$ heterointerface

Wujisiguleng Bao(包乌吉斯古楞), Sachuronggui(萨初荣贵), Fang-Yuan Qiu(仇方圆)
Chin. Phys. B . 2016, 25(12): 127102. **doi:** 10.1088/1674-1056/25/12/127102

Quantum transport properties of the three-dimensional Dirac semimetal Cd_3As_2 single crystals

Lan-Po He(何兰坡), Shi-Yan Li(李世燕)
Chin. Phys. B . 2016, 25(11): 117105. **doi:** 10.1088/1674-1056/25/11/117105

Topological nodal line semimetals

Chen Fang(方辰), Hongming Weng(翁红明), Xi Dai(戴希), Zhong Fang(方忠)
Chin. Phys. B . 2016, 25(11): 117106. **doi:** 10.1088/1674-1056/25/11/117106

RAPID COMMUNICATION

Measurement of the bulk and surface bands in Dirac line-node semimetal ZrSiS*

Guang-Hao Hong(洪光昊)[1,2,4], Cheng-Wei Wang(王成玮)[3,4], Juan Jiang(姜娟)[2,5,6], Cheng Chen(陈成)[7], Sheng-Tao Cui(崔胜涛)[2], Hai-Feng Yang(杨海峰)[2], Ai-Ji Liang(梁爱基)[2], Shuai Liu(刘帅)[2], Yang-Yang Lv(吕洋洋)[8], Jian Zhou(周健)[8], Yan-Bin Chen(陈延彬)[8], Shu-Hua Yao(姚淑华)[8], Ming-Hui Lu(卢明辉)[8], Yan-Feng Chen(陈延峰)[8], Mei-Xiao Wang(王美晓)[2], Le-Xian Yang(杨乐仙)[9], Zhong-Kai Liu(柳仲楷)[2,†], and Yu-Lin Chen(陈宇林)[2,7,9,‡]

[1] *Shanghai Institute of Optics and Fine Mechanics, Chinese Academy of Sciences, Shanghai* 201800, *China*

[2] *School of Physical Science and Technology, ShanghaiTech University and Chinese Academy of Sciences-Shanghai Science Research Center, Shanghai* 201210, *China*

[3] *Center for Excellence in Superconducting Electronics, State Key Laboratory of Functional Material for Informatics, Shanghai Institute of Microsystem and Information Technology, Chinese Academy of Sciences, Shanghai* 200050, *China*

[4] *University of Chinese Academy of Sciences, Beijing* 100049, *China*

[5] *Advanced Light Source, Lawrence Berkeley National Laboratory, Berkeley, CA* 94720, *USA*

[6] *Pohang Accelerator Laboratory, POSTECH, Pohang* 790-784, *Korea*

[7] *Department of Physics, University of Oxford, Oxford, OX*1 3*PU, UK*

[8] *National Laboratory of Solid State Microstructures, School of Physics and Department of Materials Science and Engineering, Nanjing University, Nanjing* 210093, *China*

[9] *State Key Laboratory of Low Dimensional Quantum Physics, Department of Physics and Collaborative Innovation Center of Quantum Matter, Tsinghua University, Beijing* 100084, *China*

(Received 28 October 2017; published online 1 December 2017)

Dirac semimetals are materials in which the conduction and the valence bands have robust crossing points protected by topology or symmetry. Recently, a new type of Dirac semimetals, so called the Dirac line-node semimetals (DLNSs), have attracted a lot of attention, as they host robust Dirac points along the one-dimensional (1D) lines in the Brillouin zone (BZ). In this work, using angle-resolved photoemission spectroscopy (ARPES) and first-principles calculations, we systematically investigated the electronic structures of non-symmorphic ZrSiS crystal where we clearly distinguished the surface states from the bulk states. The photon-energy-dependent measurements further prove the existence of Dirac line node along the *X*–*R* direction. Remarkably, by *in situ* surface potassium doping, we clearly observed the different evolutions of the bulk and surface electronic states while proving the robustness of the Dirac line node. Our studies not only reveal the complete electronic structures of ZrSiS, but also demonstrate the method manipulating the electronic structure of the compound.

Keywords: Dirac line-node semimetal, ZrSiS, angle-resolved photoemission spectroscopy (ARPES), bulk and surface states

PACS: 71.20.–b, 73.20.–r, 79.60.–i

DOI: 10.1088/1674-1056/27/1/017105

1. Introduction

Recently, a new type of quantum materials, so called Dirac semimetals (DSs), were discovered and intensively investigated for their rich physics and broad application potentials.[1–8] Different from regular insulators or metals, DSs are systems that host Dirac points (DPs, robust degeneracy points between conduction and valence bands) and Dirac fermions in their electronic structure and possess intriguing electronic transport behaviors such as high bulk carrier mobility and extremely large magnetoresistance.[4,5,9,10] The robustness of the Dirac points is usually protected by the crystal inversion or time reversal symmetry (e.g., in two-dimensional DS graphene[11] and three-dimensional DS Na_3Bi[2,4] and Cd_3As_2[3,5–8]). Breaking the symmetry in DS would induce a topological phase transition and achieve other nontrivial phases. For example, three-dimensional (3D) Weyl semimetal[12–16] can be realized by breaking either time reversal symmetry or inversion symmetry in 3D DS.

More recently, a new type of DSs named Dirac line-node semimetals (DLNSs) were predicted in crystals with nonsymmorphic symmetry (such as glide planes or screw axis). Unlike the previously studied DSs which contain discrete DPs, the additional symmetry in DLNSs induces and protects a

*Project supported by the National Key R&D Program of China (Grant No. 2017YFA0305400), Chinese Academy of Science–Shanghai Science Research Center (Grant No. CAS-SSRC-YH-2015-01), the National Natural Science Foundation of China (Grant No. 11674229), the Engineering and Physical Sciences Research Council Platform (Grant No. EP/M020517/1), and the Hefei Science–Center Chinese Academy of Sciences (Grant No. 2015HSC-UE013).

†Corresponding author. E-mail: liuzhk@shanghaitech.edu.cn

‡Corresponding author. E-mail: yulin.chen@physics.ox.ac.uk

© 2018 Chinese Physical Society and IOP Publishing Ltd

band degeneracy at the Brillouin zone boundary, leading to one-dimensional (1D) Dirac line nodes.[17] The degeneracy at the line node is robust against perturbations (such as spin-orbit coupling effect (SOC)). Moreover, the DLNS is predicted to host unusual electric transport properties since 1D Dirac line-nodes are a more significant feature in the band structure and can have stronger contributions to the physically observable properties of the material (e.g., in electric transport).[18–21]

The line nodes have been predicted in various compounds, including the non-symmorphic compound ZrSiS and its isostructural family WHM (W = Zr, Hf, or La; H = Si, Ge, Sn, or Sb; M = O, S, Se or Te).[22] Previous band structure measurements on ZrSiS[19,23,24] and the related compounds ZrSiTe[25] and HfSiS[26,27] by angle-resolved photoemission spectroscopy (ARPES) have found signatures of the Dirac line-nodes and the surface states. However, since the previous measurements were taken with a few discrete photon energies, a more convincing identification of the bulk and surface states and detailed measurement on the line nodes are required. Furthermore, to better investigate the transport properties originated from the Dirac line-nodes, it would be desirable to manipulate the bulk and surface electronic states including the line-node structure in ZrSiS. All of these become the goals of our work.

In this work, we systematically studied the electronic structure of ZrSiS using high-resolution ARPES with broadly tunable photon energies. The measurement across multiple BZs identified a complete set of electronic structure, including the bands coming from both the bulk and surface electronic states. Especially, we identified the Dirac line node along the X–R direction, which proves the DLNS property in ZrSiS. Moreover, by surface potassium doping, we clearly observed the different evolution behaviors of the surface and bulk bands. We further noticed that the Dirac line node remains intact after the surface doping, proving the robustness from the symmetry protection. Our finding provides detailed information on the electronic structure of ZrSiS and proposes a method for manipulating its electronic structure for future investigations and applications.

2. Experimental methods

Single crystals of ZrSiS were grown by a chemical vapor (iodine (I_2) as a transport agent) transport method in a two-step process. First, the polycrystalline ZrSiS powders were synthesized by direct solid-state reaction using high-purity elementals Zr, Si, and S in cleaned quartz ampoules. The stoichiometric amounts of ternary mixture were heated to 1100 °C and maintained at this temperature for 7 days to make the reaction complete. Then, we could obtain the single phase products after the samples were quenched to room temperature. Second, the as-prepared polycrystalline ZrSiS powder together with I_2 was sealed in a quartz tube. Then the quartz tube was kept in a two-zone furnace for 10 days with the growing temperature profile of 1150–1000 °C. The metallic luster crystals were obtained for ARPES measurements.[20]

The ARPES experiments were performed at the beamline I05 of the Diamond Light Source (DLS), beamline 10.0.1 of the Advanced Light Source (ALS) and beamline 13U of the National Synchrotron Radiation Laboratory (NSRL), Hefei, China, all of them were equipped with Scienta R4000 analyzers. The measurement sample temperature and pressure were 10 K (20 K in ALS) and lower than 1.5×10^{-10} Torr, respectively. The angle resolution was 0.2°, and the overall energy resolutions were better than 15 meV. The samples were cleaved *in situ* along the (001) plane.

The band structure and Fermi surface of bulk and slab ZrSiS were calculated by the OpenMX code[28] within the framework of the density functional theory in the generalized gradient approximation.[29] The bases are $s^3p^2d^2$, $s^2p^2d^1$, and $s^3p^3d^2f^1$ for Zr, Si, and S elements, respectively. The energy cutoff for real-space integration is 250 Ry.

3. Results and discussion

The crystal structure of ZrSiS is shown in Fig. 1(a) (PbFCl structure type in the tetragonal $P4/nmm$ space group (No. 129), with lattice constants $a = b = 3.544$ Å, $c = 8.055$ Å). In this system, square nets of Si form glide planes in the crystal, while the C_{2x} (C_{2y}) axis of the lattice is the screw axis, thus preserving two kinds of non-symmorphic symmetries.[17] The relatively weak bonding between two neighboring Zr–S layers provides a natural (001) cleavage plane. According to the *ab-initio* calculation of the bulk band structure (Fig. 1(c)), all lines along X–R direction preserve degeneracy from the protection of glide mirror, screw axis, and inversion symmetry, thus forming degenerate lines, including the Dirac line-nodes formed from the crossing of the Dirac-like band. The bulk Brillouin zone (BZ) and the surface BZ of the (001) surface are shown in Fig. 1(d) where the predicted position of the Dirac line node (solid green line) is indicated.

After cleaving, large flat and shiny surfaces are exposed, which are ideal for ARPES measurements. The high quality of the crystal can also be verified by the Laue patterns and the core level photoemission spectrum which clearly shows the characteristic Zr_{4s}, Zr_{4p}, and Si_{2p} peaks (Fig. 1(e)). The broad Fermi surface (FS) mapping in Fig. 1(f) covering multiple BZs further confirms the high quality (001) cleavage plane, which allows us to carry out the study below.

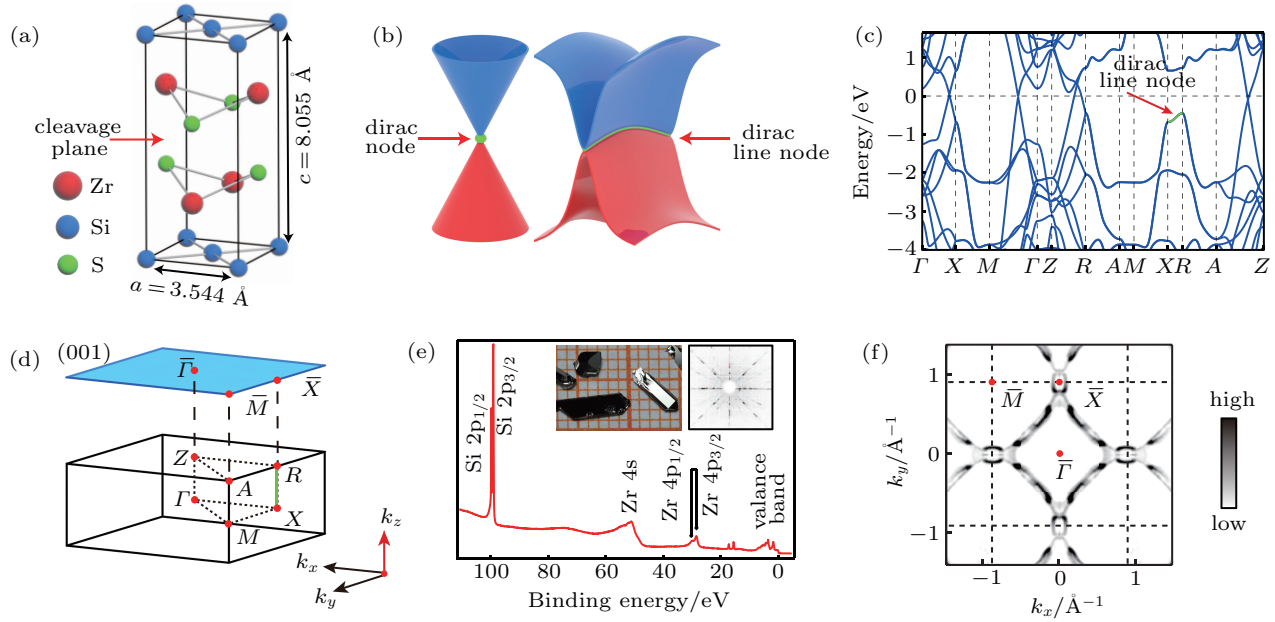


Fig. 1. (color online) Characterization of ZrSiS single crystals and Dirac line node. (a) PbFCl-type structure of ZrSiS crystal, lattice constants ($a = b =$ 3.544 Å, $c = 8.055$ Å) and cleavage plane are labelled. (b) The schematics of Dirac node and Dirac line node in the momentum space. (c) Calculation results of the bulk band structure of ZrSiS along high-symmetry directions. The green line indicates the position of the Dirac line node. (d) Illustration of the Dirac line-node location (labelled by the solid green line) in Brillouin zone boundary along the X–R direction. In addition, the projected surface BZ of (001) plane is also labelled. (e) Core level photoemission spectrum of ZrSiS showing the characteristic Zr_{4s}, Zr_{4p}, and Si_{2p} peaks. Left inset: cleaved surface of ZrSiS single crystal used in this study. Right inset: Laue pattern showing the high quality of the ZrSiS crystal. (f) Broad range photoemission spectral intensity map of the Fermi-surface covering more than one BZ, showing the correct symmetry and the characteristic of the FS.

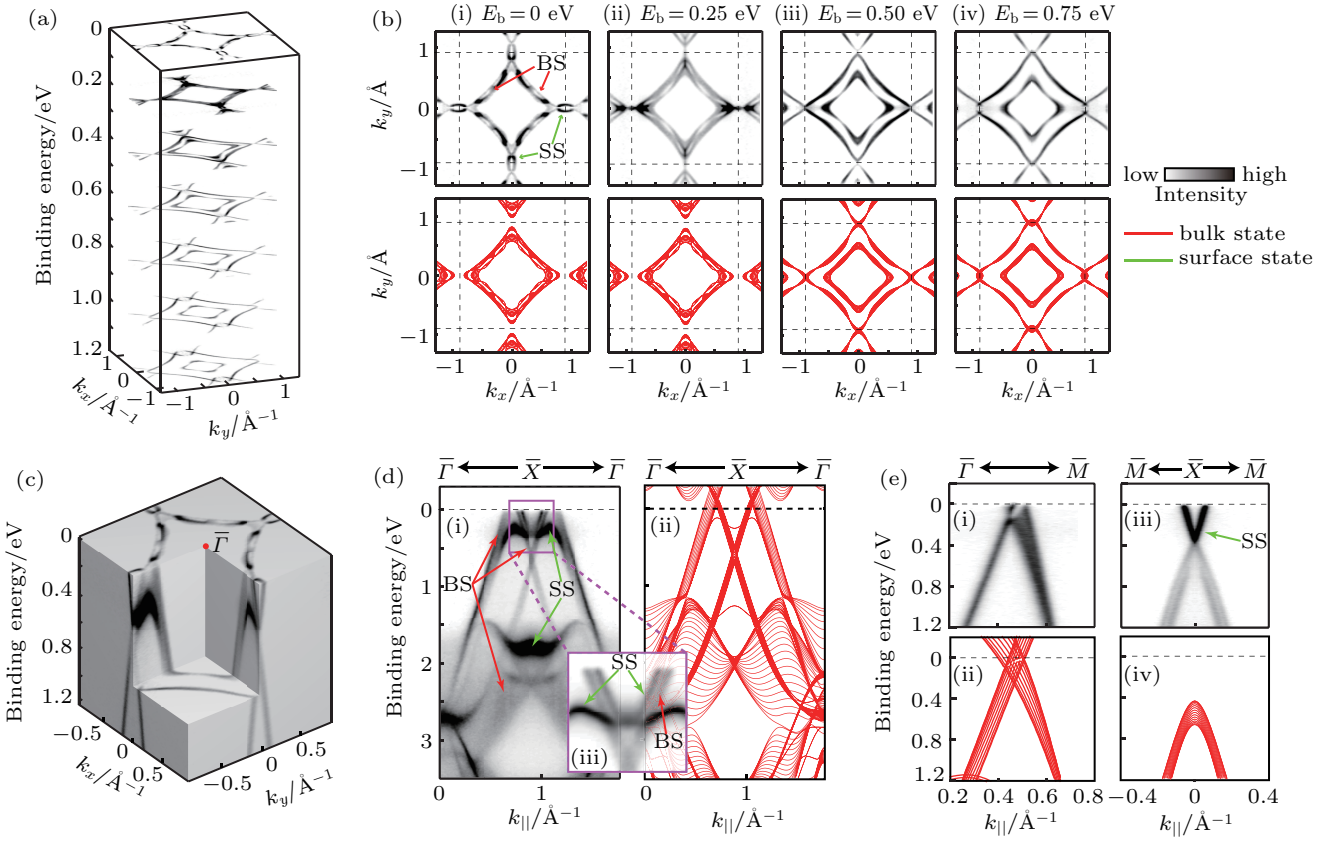


Fig. 2. (color online) General electronic structure of ZrSiS. (a) Stacking plots of constant-energy contours in broader binding energy range show the band structure evolution. (b) Top row: photoemission spectral intensity map showing the constant energy contours of bands at $E_b = 0$ eV (i), 0.25 eV (ii), 0.5 eV (iii) and 0.75 eV (iv), respectively. Bulk states (BS) and surface states (SS) are labelled. Bottom row: corresponding calculated constant energy contours at the same binding energies as in the experiments above. (c) 3D intensity plot of the photoemission spectra centred around $\bar{\Gamma}$ point. High symmetry cuts are exposed. (d) Broad range high symmetry cut along the $\bar{\Gamma}$–$\bar{X}$–$\bar{\Gamma}$ direction (i), with their corresponding calculated bulk band structure (ii). BSs and SSs are labelled on the data and zoomed in surface states near the Fermi level (iii). (e) High symmetry cuts along the $\bar{\Gamma}$–$\bar{M}$ (i) and $\bar{M}$–$\bar{X}$–$\bar{M}$ (iii) directions and corresponding calculated bulk band structures ((ii), (iv)). SS is labelled in the data.

To investigate the detailed electronic structure of ZrSiS, we focus on the first BZ by carrying out high-resolution ARPES measurements, and the results are shown in Fig. 2. The stacking plots of constant-energy contours in a broader binding energy range (Fig. 2(a)) show the electronic structure evolution around the $\bar{\Gamma}$ point. From the detailed plot of the constant energy contours (Fig. 2(b)), we could clearly identify two sets of features: one is the large diamond-shaped FS, which is formed by the connected band structure at four $\bar{X}$ points; the other is the elliptical electronic pocket centered at each $\bar{X}$ point. While the first set of features can be well reproduced by our *ab-initio* calculations of the bulk bands (Figs. 2(b)(i)–2(b)(iv)), the second set of features could not be found in the bulk band calculations, suggesting their bulk and surface origins, respectively.

In addition to the constant energy contours, we focus on the dispersions along the high symmetry directions (Figs. 2(c)–2(e)). We compare the bulk bands between experiments and *ab-initio* calculations along the high symmetry directions ($\bar{\Gamma}$–$\bar{X}$–$\bar{\Gamma}$, $\bar{\Gamma}$–$\bar{M}$, and $\bar{M}$–$\bar{X}$–$\bar{M}$), the excellent overall agreement allows us to identify the surface states (the observed bands not included in the bulk band calculations, as indicated by the green arrows in Figs. 2(d)(i) and 2(e)(iii)) from the bulk states (red solid curves in Figs. 2(d)(i) and 2(e)(iii)). Combining the constant-energy contours, we notice that the surface states form a parabolic shape around the $\bar{X}$ point, while the bulk band dispersions (Fig. 2d(i)) form a linear crossing (Dirac point) sitting at $E_b \approx 0.53$ eV at the $\bar{X}$ point. Furthermore, we notice a small gap opening at the band crossing along the $\bar{\Gamma}$–$\bar{M}$ direction due to the effect of SOC, showing nice agreement with the *ab-initio* calculations (Fig. 2(e)(ii)).

The surface and bulk nature of the electronic bands are further supported by the photon-energy-dependent measurement which probes the band dispersion at different k_z values. By a series of measurements at different photon energies, we clearly identify the surface and bulk bands in the FS at $k_y k_z$ momentum space (Fig. 3(a)). For details, we choose four cuts and plot them in Figs. 3(b)(i)–3(b)(iv) with their respective k_z locations indicated by the magenta dotted lines ($15\pi/c$ to $16\pi/c$) in Fig. 3(a). We clearly notice that while the parabolic type bands do not change with k_z, other features show variation with k_z, proving their origins from the surface and bulk, respectively. Moreover, we clearly observe that the Dirac node formed by linear band touching disperses with k_z and results in a line-node along the X–R direction (Figs. 3(c) and Fig. 3(d)). With measurements of fine k_z steps, the dispersion of the X–R line node could be reconstructed (by tracking the positions of the DP positions), as illustrated in Fig. 3(e), which shows good agreement with our calculations (solid green curve in Fig. 3(e)).

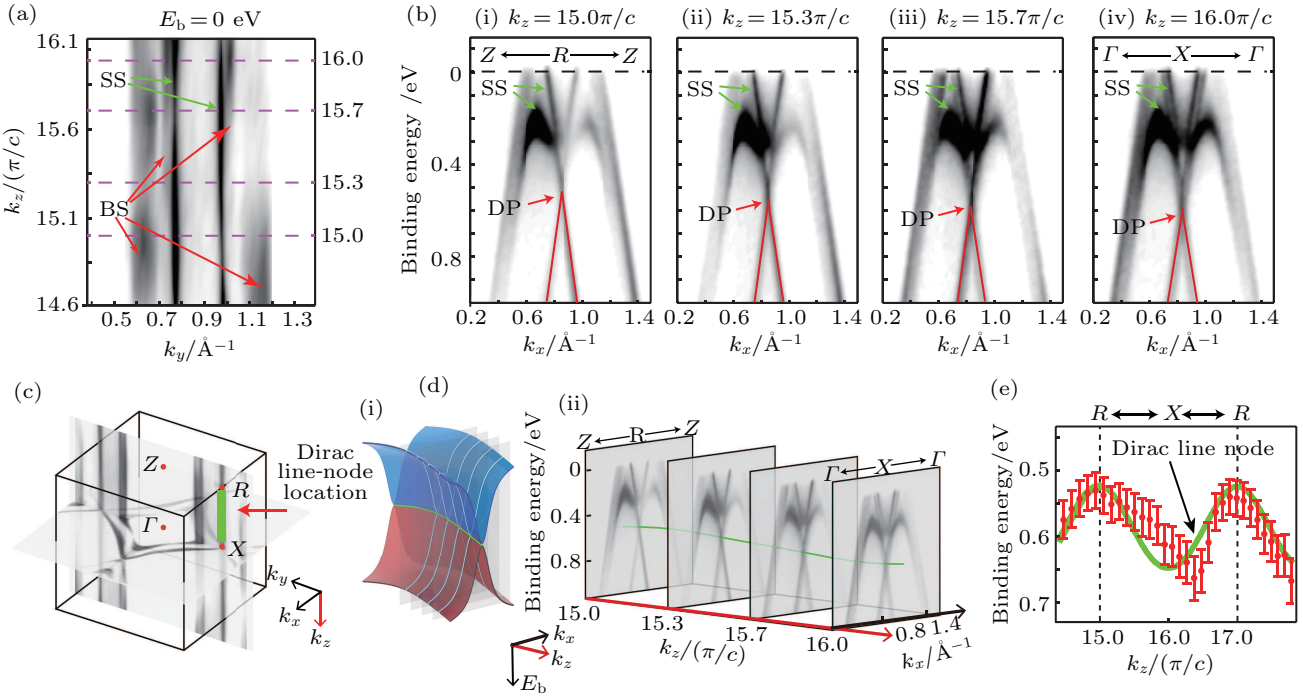


Fig. 3. (color online) K_z measurements and Dirac line node in ZrSiS. (a) Plot of the constant energy contour at E_F in k_y–k_z space. The bulk and surface state bands are indicated by the red and green arrows, respectively. Magenta dotted lines indicate the k_z positions of four representing cuts shown in (b) and (d). (b) Detailed analysis of the four representing cuts, the surface bands and linear dispersions are marked. (c) The 3D BZ shows the constant energy contours (k_y–k_z plane and k_x–k_y plane) around the DP and illustrates the location of the Dirac line node (green solid line) in ZrSiS (X–R direction). (d) (i) Schematic of the Dirac line node along the k_z direction (labelled by the green curve) with the grey planes which are corresponding to each cut in (b) and (d) (ii). The bright curves sketch the Dirac dispersions we observe in each cut as in (ii). (ii) Stack plot of the four cuts as in (b). Green curve indicates the dispersion of the Dirac line node. (e) The fitted DP positions (red dots) at various k_z values, the green curve indicates the calculated dispersion along the X–R direction.

Finally, we demonstrate the modification of the electronic structure of ZrSiS by introducing alkaline metal onto the sample surface. The stacking plots of constant-energy contours (Fig. 4(a)) show the electronic structure evolution after surface potassium doping. By comparing the FS and high symmetry cuts ($\bar{\Gamma}$–$\bar{X}$–$\bar{\Gamma}$ and $\bar{M}$–$\bar{X}$–$\bar{M}$) (Figs. 4(b)–4(d)), we clearly see that the bands identified as surface state bands shift away from $E_{\rm F}$ significantly and change their shape and volume while the bulk state bands almost do not show much shift or change. Such different behaviors not only help us clearly identify the surface states bands and bulk states bands, but also demonstrate the effect of tuning the surface and bulk electronic structures in ZrSiS. Moreover, as the surface dopant appears as perturbative impurities, the fact that the Dirac point stays intact proves the robustness of the Dirac line-node under the protection of the non-symmorphic crystal symmetry.

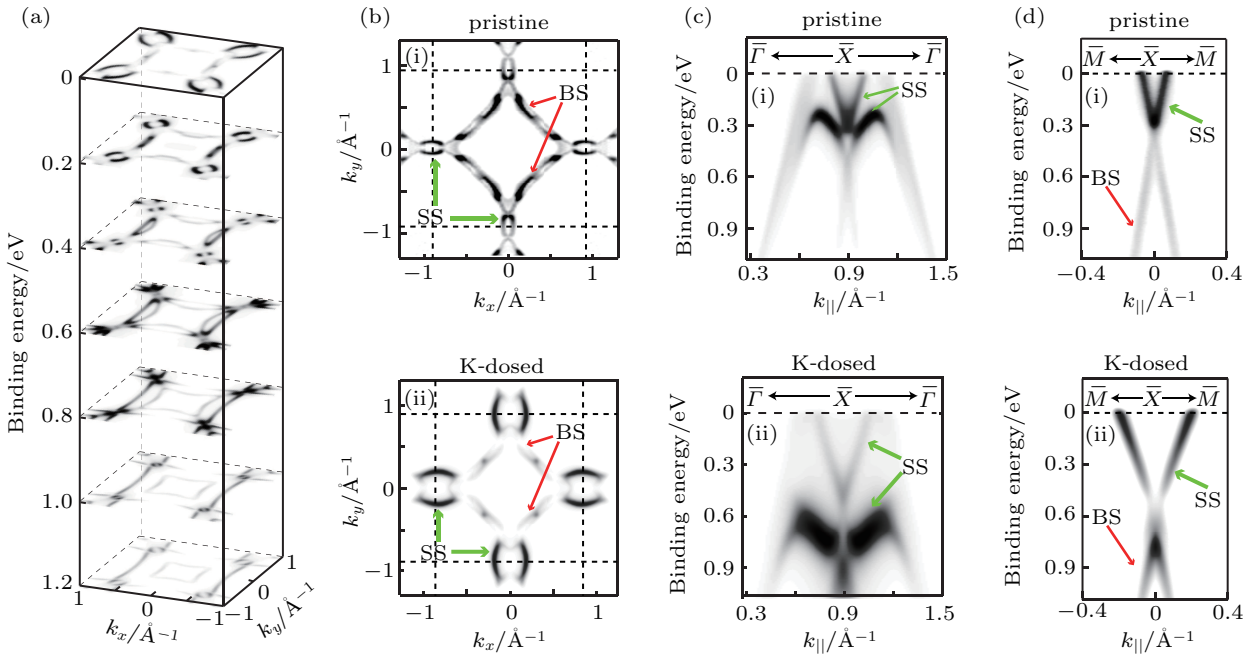


Fig. 4. (color online) Surface potassium doping results in ZrSiS. (a) Stacking plots of constant-energy contours in broader binding energy range in the K-doped sample. (b) Side-by-side comparison of (i) pristine and (ii) K-dosed data on the Fermi surface where we can easily distinguish SSs from the BSs. (c) Side-by-side comparison of the high symmetry cut along $\bar{\Gamma}$–$\bar{X}$–$\bar{\Gamma}$ direction in the (i) pristine and (ii) K-dosed sample where the SSs are labelled. (d) Side-by-side comparison of the high symmetry cuts along $\bar{M}$–$\bar{X}$–$\bar{M}$ direction in the (i) pristine and (ii) K-dosed sample where the SSs and BSs are labelled.

4. Conclusion and perspectives

In summary, our systematic measurement of the electronic structure of the ZrSiS compound has obtained the full set of band structure in the BZ, including the electronic states originated from both the bulk and surface. Our measurement of the Dirac line node convincingly establishes that ZrSiS is a DLNS protected by non-symmorphic symmetry. Our *in-situ* K-doping data illustrates the different behaviors of the surface and bulk bands, as well as the robustness of the Dirac line-node. These band characteristics not only help us understand the intriguing transport properties in ZrSiS, but also point to methods in manipulating the electronic properties in DLNS.

References

[1] Young S M, Zaheer S, Teo J C Y, Kane C L, Mele E J and Rappe A M 2012 *Phys. Rev. Lett.* **108** 140405

[2] Wang Z J, Sun Y, Chen X Q, Franchini C, Xu G, Weng H M, Dai X and Fang Z 2012 *Phys. Rev. B* **85** 195320

[3] Wang Z J, Weng H M, Wu Q S, Dai X and Fang Z 2013 *Phys. Rev. B* **88** 125427

[4] Liu Z K, Zhou B, Zhang Y, Wang Z J, Weng H M, Prabhakaran D, Mo S K, Shen Z X, Fang Z, Dai X, Hussain Z and Chen Y L 2014 *Science* **343** 864

[5] Liu Z K, Jiang J, Zhou B, Wang Z J, Zhang Y, Weng H M, Prabhakaran D, Mo S K, Peng H, Dudin P, Kim T, Hoesch M, Fang Z, Dai X, Shen Z X, Feng D L, Hussain Z and Chen Y L 2014 *Nat. Mater.* **13** 677

[6] Neupane M, Xu S Y, Sankar R, Alidoust N, Bian G, Liu C, Belopolski I, Chang T R, Jeng H T, Lin H, Bansil A, Chou F and Hasan M Z 2014 *Nat. Commun.* **5** 3786

[7] Ali M N, Gibson Q, Jeon S, Zhou B B, Yazdani A and Cava R J 2014 *Inorg. Chem.* **53** 4062

[8] Borisenko S, Gibson Q, Evtushinsky D, Zabolotnyy V, Buchner B and Cava R J 2014 *Phys. Rev. Lett.* **113** 027603

[9] Feng J Y, Pang Y, Wu D S, Wang Z J, Weng H M, Li J Q, Dai X, Fang Z, Shi Y G and Lu L 2015 *Phys. Rev. B* **92** 081306

[10] Liang T, Gibson Q, Ali M N, Liu M H, Cava R J and Ong N P 2015 *Nat. Mater.* **14** 280

[11] Castro Neto A H, Guinea F, Peres N M R, Novoselov K S and Geim A K 2009 *Rev. Mod. Phys.* **81** 109

[12] Zyuzin A A, Wu S and Burkov A A 2012 *Phys. Rev. B* **85** 165110

[13] Weng H M, Fang C, Fang Z, Bernevig B A and Dai X 2015 *Phys. Rev. X* **5** 011029

[14] Xu S Y, Belopolski I, Alidoust N, *et al.* 2015 *Science* **349** 613

[15] Lv B Q, Xu N, Weng H M, Ma J Z, Richard P, Huang X C, Zhao L X, Chen G F, Matt C E, Bisti F, Strocov V N, Mesot J, Fang Z, Dai X, Qian T, Shi M and Ding H 2015 *Nat. Phys.* **11** 724

[16] Yang L X, Liu Z K, Sun Y, Peng H, Yang H F, Zhang T, Zhou B, Zhang Y, Guo Y F, Rahn M, Prabhakaran D, Hussain Z, Mo S K, Felser C, Yan B and Chen Y L 2015 *Nat. Phys.* **11** 728

[17] Young S M and Kane C L 2015 *Phys. Rev. Lett.* **115** 126803

[18] Singha R, Pariari A K, Satpati B and Mandal P 2017 *Proc. Natl. Acad. Sci. USA* **114** 2468

[19] Wang X F, Pan X C, Gao M, Yu J H, Jiang J, Zhang J R, Zuo H K, Zhang M H, Wei Z X, Niu W, Xia Z C, Wan X G, Chen Y L, Song F Q, Xu Y B, Wang B G, Wang G H and Zhang R 2016 *Adv. Electron. Mater.* **2** 1600228

[20] Lv Y Y, Zhang B B, Li X, Yao S H, Chen Y B, Zhou J, Zhang S T, Lu M H and Chen Y F 2016 *Appl. Phys. Lett.* **108** 244101

[21] Kumar N, Manna K, Qi Y P, Wu S C, Wang L, Yan B H, Felser C and Shekhar C 2017 *Phys. Rev. B* **95** 121109

[22] Xu Q N, Song Z D, Nie S M, Weng H M, Fang Z and Dai X 2015 *Phys. Rev. B* **92** 205310

[23] Neupane M, Belopolski I, Hosen M M, Sanchez D S, Sankar R, Szlawska M, Xu S Y, Dimitri K, Dhakal N, Maldonado P, Oppeneer P M, Kaczorowski D, Chou F C, Hasan M Z and Durakiewicz T 2016 *Phys. Rev. B* **93** 201104

[24] Schoop L M, Ali M N, Strasser C, Topp A, Varykhalov A, Marchenko D, Duppel V, Parkin S S P, Lotsch B V and Ast C R 2016 *Nat. Commun.* **7** 11696

[25] Topp A, Lippmann J M, Varykhalov A, Duppel V, Lotsch B, Ast C R and Schoop L M 2016 *New. J. Phys.* **18** 125014

[26] Chen C, Xu X, Jiang J, *et al*. 2017 *Phys. Rev. B* **95** 125126

[27] Takane D, Wang Z W, Souma S, Nakayama K, Trang C X, Sato T, Takahashi T and Ando Y 2016 *Phys. Rev. B* **94** 121108

[28] http://www.openmx-square.org.

[29] Perdew J P, Burke K and Ernzerhof M 1996 *Phys. Rev. Lett.* **77** 3865